Design Optimization of a Rotor for Flywheel Energy Storage System

Kainat Riaz, Syeda Fatima Imam, Zia ul Rehman Tahir(✉), Tariq Ali, Ahmad Hassan, Imran Amin, Nida Ilyas, Muhammad Taimoor Adil, Sajeer Ahmad, Muhammad Abdullah, Najum ud Din, and Muhammad Saad

Department of Mechanical Engineering, University of Engineering and Technology Lahore, Lahore, Pakistan
ziartahir@uet.edu.pk

Abstract. The aim of this study is to design and shape optimization of flywheel rotor with different combinations of diameter and height with constant rotational speed, energy storage capacity and material properties. Shape optimization was performed for three different shapes to find the most suitable shape for rotor. The suitable combinations of rotor height and diameter of optimized shape were determined for maximum energy storage value within commercially available range. A static analysis was conducted to calculate stresses and deformations for combinations of rotor height and radius and the best combination was selected based on lowest value of stress and deformation. The narrowed down limits of these values were used for second optimization to increase precision. The intersecting combinations of diameter and height were used as input in third optimization. The final model was obtained by converging dimensions from each case experiencing the least stress and displacement. The model height 889.3 mm and outer diameter 377.1 mm had optimum deflection and minimum stress.

Keywords: Flywheel energy storage systems · Shape optimization · Flywheel rotor design · Optimum radius to height ratio

1 Introduction

Flywheel Energy Storage System (FESS) is a renewable energy storage device that provides instantaneous power, reduced carbon emissions, a longer lifetime, larger efficiency, and high charging and discharging rates [1]. FESS is an environment-friendly system as no harmful substance is involved in its functioning and has no carbon footprint. For short time durations, the flywheel has become a feasible means for frequency regulation, voltage levelling, and fault ride-through support of intermittent sources such as wind and solar farms [2].

The power and energy are independent of the system delivered by FESS. The energy provided by FESS is determined by the material, size of the rotor, and rotational speed. The power rating of FESS is dictated by the electronics being used in the system, for example, the motor/generator [3, 4]. Flywheels can provide both continuous and pulsed

P. Schossig et al. (Eds.): IRES 2022, AHE 16, pp. 422–433, 2023.
https://doi.org/10.2991/978-94-6463-156-2_27

power to the different subsystem controls and power-conditioning devices on the vehicle distribution networks [5].

A flywheel rotor is a mechanical component that rotates at a certain velocity with a certain mass that can store energy by its speed and mass [6]. Under normal operation, the deceleration of the rotor is about half of its maximum speed. To minimize the energy losses due to friction, vacuum enclosure and magnetic bearing system are frequently used [7]. Radial stresses of flywheel rotors can be reduced by a properly designed hub construction. Ha, Kim et al. [8] proposed a hub structure that is separated at numerous points along its length. The required radial compressive load can be imposed on the inside surface of the rotor by the sections of the hub. Hu et al. [9] observed that if rotor rotational speed exceeds its critical limits, its behaviour gyroscopically affects the model resulting in various degrees of deformation and mechanical failure.

The Shape factor (K) mainly depends on the rotor geometry. Metal rotors can be fabricated for high shape factors. The selection of material rotors also depends on the shape factor [10, 11]. In this study, steel has been chosen as the rotor material as it is cheaper and much more easily available than fibre materials. In past research, no such analysis or optimization of steel rotors has been done.

The first objective of this study is to compute optimum diameter and height of cylindrical rotor of FESS which can deliver the power of 50 kW at 50,000 rpm with a retention time of 1 h. The deflection and von Mises stress are used to find optimum height and diameter. The second objective is to optimize dominating cylindrical shape by slight variation in diameter and height.

2 Methodology

A literature review was carried out to study shapes used for rotor of flywheel energy storage system. The shapes commonly used in the recent literature are: cylindrical, conical, laval and oval. A stress analysis to be performed for these shapes by keeping inner diameter, outer diameter, height and material (Steel) same to find shape having lower von Mises stress.

To achieve one of objective geometric optimization for cylindrical shape is to be performed for rotor to store power of 50 kW for a retention time of one hour. The required energy to store by the flywheel is 180 MJ. The energy storage capacity of a rotor is calculated using Eq. (1), ρ is density of material, ω is rotational speed, R and H are outer radius and height of the rotor respectively. The factor R^4H is required to optimize for minimum stress and deflection.

$$E = \frac{\pi}{4}\rho R^4 H \omega^2 \tag{1}$$

A literature review was carried out to find range of diameter and height of commercially available flywheel energy system having energy storage capacity around 180 MJ, the range diameter and height of the rotors is 300–1200 mm and 10–2080 mm respectively.

A geometric optimization of cylindrical shape was performed to find optimum diameter and height of the rotor for 180 MJ of energy, this optimization is named as Step

1. The diameter was varied from 1200 to 300 mm with step size of 20 mm and height was varied from 10 to 2100 mm with step size of 10 mm. The energy for each diameter using all heights was calculated. The combinations of diameter and height for required energy was selected. A numerical analysis was performed to compute maximum stress and maximum deflection for each combination.

The maximum stress and maximum deflection for each combination was to find optimized range of diameter and height. This rage with step size of 1 mm was used for stage 2 optimization to calculate required energy. This process was repeated with step size of 0.1 mm for optimization stage 3. Commercial finite element analysis package Abaqus was used to perform numerical analysis to compute maximum von Mises stress and deflection of the rotor. Optimize diameter and height of the rotor was computed using three stages of optimization.

The optimize diameter and height of the rotor was further used to find optimized cylindrical shape. Three cases for varying height and diameter were used for this purpose. Case A, by keeping diameter and height at inner diameter constant, and varying height at outer diameter as $\pm 15\%$ of original height. Case B, by keeping height and diameter at edges constant, and varying diameter at mid-height as $\pm 5\%$ of original diameter. Case C, by keeping diameter and height at edges constant, and varying height at mean diameter as $\pm 15\%$ of original height. The geometry of these models was created in SolidWorks and then imported in Abaqus for analysis.

3 Results and Discussion

3.1 Shape Selection

Four shapes are commonly reported in the literature for rotor of flywheel used for energy storage systems, the shapes are: Cylindrical, Conical, Laval and Oval. An analysis was performed on four shapes to compute von Mises stresses by keeping inner diameter, outer diameter, height and material (Steel) same. The von Mises stress for cylindrical, conical, laval and oval shapes is 9.7, 25.0, 22.5 and 14.3 MPa respectively. The cylindrical shape is the most suitable among four as it gave minimum von Misses stresses and used for further analysis.

3.2 Numerical Model

The numerical model used in the analysis was a hollow cylindrical shape with fixed inner diameter (90 mm). The geometry was created in SolidWorks and then imported to Abaqus for analysis. The section was selected as *Solid Homogenous.* The material was selected as steel with density, modulus of elasticity and Poisson's ratio as 7850 kg.m3, 200 GPa and 0.3 respectively.

The boundary condition type *Displacement/Rotation* was selected, all translational displacements were set to zero, rotational displacements perpendicular to radial and tangential direction were set to zero. The rotational displacement perpendicular to axial direction was allowed. A load of 5236 rad/sec was applied to the whole rotor as rotational body force keeping uniform distributions.

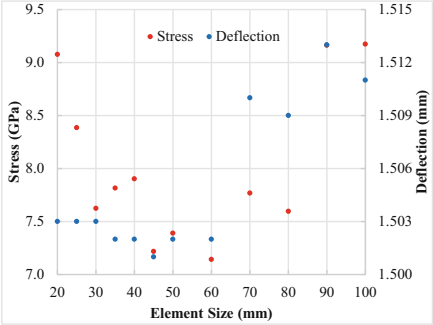

Fig. 1. Element size versus maximum von mises stress and maximum deflection

The mesh sensitivity analysis of the numerical model was performed for different global element size. The tetrahedron element shape with free meshing technique was used. A 10-node quadratic tetrahedron element type was selected. The element size was changed from 100 to 20 mm, the maximum von Mises stress and maximum deflection for each element size is presented in Fig. 1. There is general trend of decrease in maximum defection with decrease in element size. The maximum von Mises stress decrease generally with decrease in element size and then stress increase with further decrease in element size. The optimum element size is in between 45 to 60 mm, so element size of 50 mm was selected for further analysis.

3.3 Geometry Optimization Step 1

The cost function for optimization of geometry of cylinder was set as 180 MJ energy storage capacity. The diameter of the cylinder was varied from 300 mm to 1200 mm with step of 20 mm and height of the cylinder was varied from 10 mm to 2100 mm with step of 10 mm. The energy storage capacity of all commination was calculated and 14 combinations having energy storage capacity of more than 180 MJ were selected. These combinations are designated as Model S1-1 to S1-14, diameters and heights for the combinations are presented in Table 1. Model S1-1 to S1-14 were analysed in Abaqus, maximum stress and maximum deflection for these models are presented in Table 1.

The maximum von Mises stress versus diameter and height for 14 models are presented in Fig. 2 (a). The stress increase with increase in diameter whereas decreases with increase in height. The maximum deflection versus diameter and height for 14 models are presented in Fig. 2 (b). Figure 2 (a) shows with the increases in height the stresses in the flywheel decrease, the inverse relationship can be explained by the fact that as the height of a body increases the stiffness and resisting area for applied load also increases. On the other hand, as diameter increases the stresses also increase as shown in Fig. 2 (b), the reason is as the diameter increases the body is more prone to cracks and residual stresses [12].

The curves for stress and diameter pass close to each other at diameter from 300 to 400 mm and height from 900 to 1200 mm. The intersecting range of height and diameter were used for further optimization.

Table 1. Height and diameter combinations for Step 1 Optimization

Model	Diameter (mm)	Height (mm)	Stress (GPa)	Deflection (mm)
S1–1	320	1710	5.49	0.903
S1–2	340	1340	6.169	1.124
S1–3	360	1070	7.08	1.372
S1–4	380	860	7.84	1.623
S1–5	400	700	8.10	1.857
S1–6	420	570	8.98	2.049
S1–7	440	470	9.446	2.206
S1–8	460	400	10.05	2.358
S1–9	480	330	10.78	2.524
S1–10	500	280	12.02	2.808
S1–11	520	240	11.94	3.202
S1–12	540	210	12.15	3.634
S1–13	560	180	12.75	4.086
S1–14	620	120	13.73	5.589

3.4 Geometry Optimization Step 2

The geometry optimization Step 2 of the rotor was performed for range for diameter from 360 to 380 mm and range of height from 860 to 1070 mm. The step of diameter and height was used as 1 mm. The energy of all combinations was calculated and 11 combinations of diameter and height with energy more than 180 MJ were selected. The numerical models are designated as S2–1 to S2–11 and are presented in Table 2.

The numerical analysis using Abaqus for models S2–1 to S2–11 is performed, maximum stress and maximum deflection is presented in Table 2. The maximum von Mises stress versus height and diameter is presented in Fig. 3 (a). The maximum deflection versus height and diameter is presented in Fig. 3 (b).

The deflection shows an almost linear trend for both height and diameter as shown in Fig. 3 (b). The deflection decreases with increasing height and increases with increasing diameter. There is general trend of increase in stress with increasing diameter and decreasing height but there are some discontinuities in both curves.

The curves for deflection pass close to each other at diameter from 368 to 372 mm and height from 950 to 1000 mm. The curves for stress pass close to each other at diameter from 368 to 372 mm and height from 950 to 1000 mm. There is discontinuity in the curve stress versus diameter for diameter from 372 to 376 mm, and there is discontinuity in the curve stress versus height for height from 900 to 950 mm. The intersecting range of height and diameter considering discontinuity were used for further optimization.

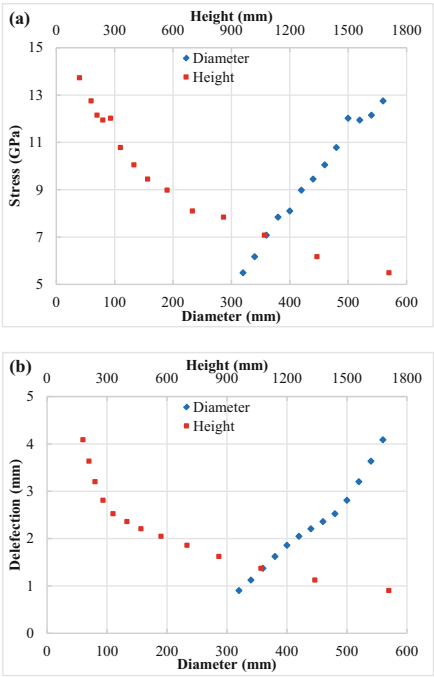

Fig. 2. Height and diameter of rotor for stage 1 optimization versus (a) stress, (b) deflection

Table 2. Height and diameter combinations for Step 2 Optimization

Model	Diameter (mm)	Height (mm)	Stress (GPa)	Deflection (mm)
S2–1	360	1070	7.080	1.300
S2–2	362	1047	6.631	1.320
S2–3	364	1024	6.753	1.340
S2–4	366	1002	6.859	1.370
S2–5	368	980	6.919	1.390
S2–6	370	959	7.058	1.420
S2–7	372	939	7.207	1.450
S2–8	374	919	7.138	1.470
S2–9	376	899	7.581	1.490
S2–10	378	880	7.700	1.520
S2–11	380	862	7.783	1.540

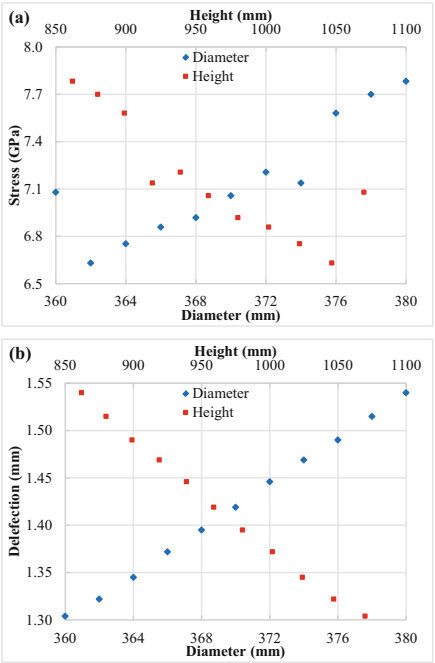

Fig. 3. Height and diameter of rotor for stage 2 optimization versus (a) stress, (b) deflection

3.5 Geometry Optimization Step 3

The geometry optimization Step 3 of the rotor was performed for range for diameter from 368 to 380 mm and range of height from 860 to 1000 mm. The step of diameter and height was used as 0.1 mm. The energy of all combinations was calculated and 11 combinations of diameter and height with energy more than 180 MJ were selected. The numerical models are designated as S3–1 to S3–11 and are presented in Table 3. The numerical model presented in Table 3 were analysed in Abaqus, the maximum deflection and maximum stress is presented in Table 3.

The maximum deflection versus height and diameter for numerical models S3–1 to S3–11 are presented in Fig. 4 (a). There is general trend of increase in deflection with increasing diameter and deceasing height with some exception around diameter of 377 mm and height of 890 mm. The numerical model S3–6 showed exception for both trends of stress and deflection.

The maximum von Mises stress versus height and diameter for numerical models od stage 3 are presented in Fig. 4 (a). There is no general trend of variation of stress with diameter and height. The numerical model S3–6 showed lowest stress among all numerical models. The numerical model S3–6 with heigh of 889.3 and diameter of 377.1 gave lowest values of stress and deflection for models of step 3 optimization so this model is optimized model for given energy storage capacity.

Table 3. Height and diameter combinations for Step 3 Optimization

Model	Diameter (mm)	Height (mm)	Stress (GPa)	Deflection (mm)
S3–1	376.0	899.0	7.581	1.490
S3–2	376.2	897.9	7.678	1.495
S3–3	376.4	895.9	7.633	1.498
S3–4	376.6	894.0	7.468	1.500
S3–5	376.8	892.2	7.713	1.503
S3–6	377.1	889.3	7.390	1.502
S3–7	377.2	888.3	7.623	1.506
S3–8	377.4	886.5	7.645	1.510
S3–9	377.6	884.4	7.668	1.513
S3–10	377.8	882.7	7.753	1.514
S3–11	378.0	880.9	7.665	1.517

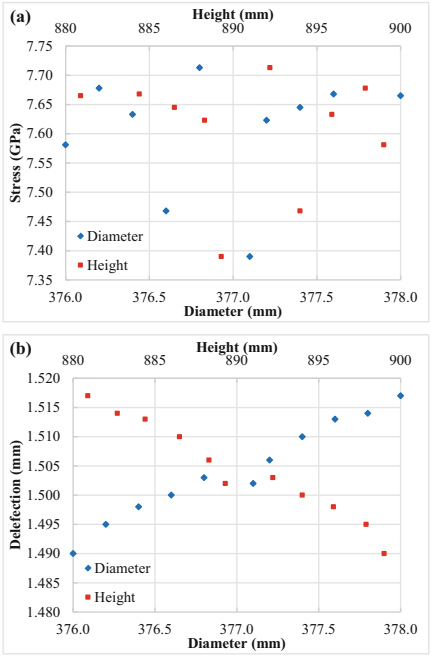

Fig. 4. Height and diameter of rotor for stage 3 optimization versus (a) stress, (b) deflection

3.6 Shape Optimization

The model S3–6 with height 889.3 mm and outer diameter 377.1 mm had optimum deflection and minimum stress. This model is taken as *Reference* for shape optimization.

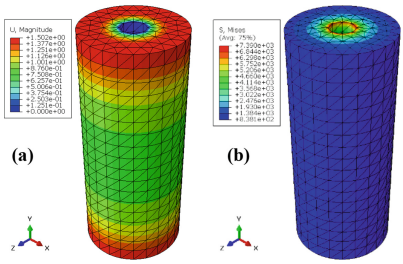

Fig. 5. Contour plot of Model M3–6 for (a) Deflection (b) von Mises stress

The maximum deflection and maximum von Mises stress for this model is shown in Fig. 5.

The cylindrical shape with length and outer diameter for reference model is further optimize for shape for four cases.

Case A, keeping outer diameter and height at inner diameter constant, and varying height at outer diameter as ±15% of original height. The numerical models were designated as A01 to A11, numerical models A01 and A11 are shown in Fig. 5 (a) and 5 (b) respectively. The maximum stress and maximum defection for case A is presented in Table 4.

Case B, keeping height and diameter at edges constant, and varying diameter at midheigh as ±15% of original diameter. The numerical models were designated as B01 to

Table 4. Shape optimization of rotor

Case A: Constant diameter, inner height constant and varying outer height (±15%)			
Model	Height (mm)	Stress (GPa)	Deflection (mm)
A01	755.910	4.837	1.036
Reference	889.300	7.390	1.502
A11	1022.700	23.87	2.895
Case B: Constant height and varying diameter along mid-height (±15%)			
Model	Diameter (mm)	Stress (GPa)	Deflection (mm)
C01	320.535	6.450	1.332
Reference	377.100	7.390	1.502
C11	433.660	8.869	1.780
Case C: Constant diameter and varying height along mean diameter (±15%)			
Model	Height (mm)	Stress (GPa)	Deflection (mm)
D01	822.6	4.530	2.076
Reference	889.3	7.390	1.502
D11	956.0	10.460	1.725

B11, numerical models B01 and B11 are shown in Fig. 5 (c) and 5 (d) respectively. The maximum stress and maximum defection for case B is presented in Table 4.

Case C, keeping height and diameter constant, and varying height at mean diameter as ±15% of original height. The numerical models were designated as D01 to D11, numerical models C01 and C11 are shown in Fig. 5 (e) and 5 (f) respectively. The maximum stress and maximum defection for case C is presented in Table 4.

The model from each case (Case A, Case B and Case C) with lowest values of stresses and deflection was selected and converged into a single model. The diameter and outer height of this model were 377.1 mm and 1022.7 mm respectively. The rotor had a hub diameter of 90 mm and its inner height was 755.91 mm. The lower and upper cylindrical surfaces of the rotor were converged inwards at 882.6 mm.

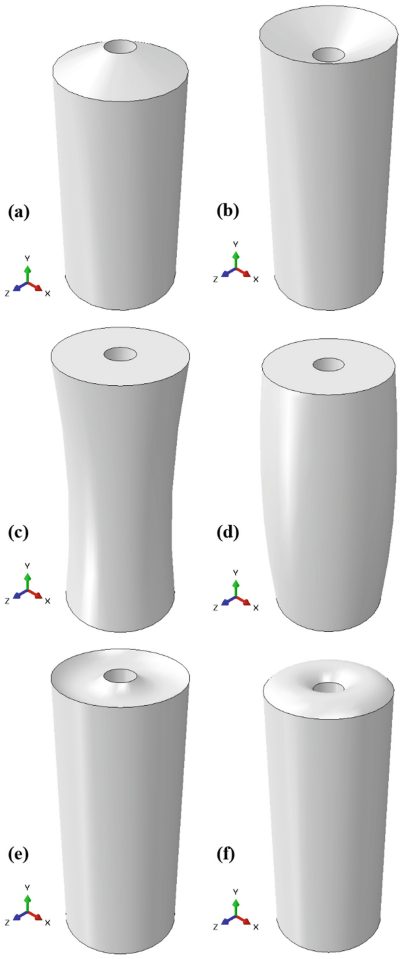

Fig. 6. Shape modification to reference model (a) Case A with − 15%, (b) Case A with +15%, (c) Case B with − 15%, (d) Case B with +15%, (e) Case C with − 15%, (f) Case D with +15%

4 Conclusions

The shape optimization of rotor of Flywheel Energy Storage System (FESS) is presented in this study. The range of diameter and height of rotor having energy storage capacity of 180 MJ were selected by reviewing literature. The optimum diameter and height of the rotor was computed using minimum stress and minimum deflection for three stages of geometric optimization. The model height 889.3 mm and outer diameter 377.1 mm had optimum deflection and minimum stress. The shape optimization of cylindrical rotor was performed for three cases by slightly varying diameter and height to keep dominated cylindrical shape.

Acknowledgments. The authors would like to acknowledge Department of Mechanical Engineering, University of Engineering and Technology, Lahore for providing computer facilities used for this study.

Authors' Contributions. **Kainat Riaz:** Original Draft Writing, Formal Analysis.
Syeda Fatima Imam: Original Draft Writing, Formal Analysis.
Zia ul Rehman Tahir: Conceptualization, Methodology, Investigation, Validation.
Tariq Ali: Writing, Review/Editing, Formatting.
Ahmad Hassan: Review/Editing,
Imran Amin: Review/Editing, Formatting.
Nida Ilyas: Original Draft Writing, Formal Analysis.
Muhammad Taimoor Adil: Methodology, Investigation, Validation, Writing.
Sajeer Ahmad: Writing, Review/Editing.
Muhammad Abdullah: Writing, Review/Editing.
Najum ud Din: Review/Editing.
Muhammad Saad: Review/Editing.

References

1. Okou, R., et al., *The potential impact of small-scale flywheel energy storage technology on Uganda's energy sector %J Journal of Energy in Southern Africa.* 2009. **20**: p. 14–19.
2. Arani, A.A.K., et al., *Review of Flywheel Energy Storage Systems structures and applications in power systems and microgrids.* Renewable and Sustainable Energy Reviews, 2017. **69**: p. 9-18.
3. Hadjipaschalis, I., A. Poullikkas, and V. Efthimiou, *Overview of current and future energy storage technologies for electric power applications.* Renewable and Sustainable Energy Reviews, 2009. **13**(6): p. 1513-1522.
4. Hebner, R., J. Beno, and A. Walls, *Flywheel batteries come around again.* IEEE Spectrum, 2002. **39**(4): p. 46-51.
5. Arnold, S.M., A.F. Saleeb, and N.R. Al-Zoubi, *Deformation and life analysis of composite flywheel disk systems.* Composites Part B: Engineering, 2002. **33**(6): p. 433-459
6. Genta, G., *Kinetic energy storage: theory and practice of advanced flywheel systems.* 2014: Butterworth-Heinemann.
7. Krack, M., M. Secanel, and P.J.J.O.A.M. Mertiny, *Advanced optimization strategies for cost-sensitive design of energy storage flywheel rotors.* 2011. **43**(2): p. 65–78.

8. Ha, S.K., et al., *Design and Spin Test of a Hybrid Composite Flywheel Rotor with a Split Type Hub.* Journal of Composite Materials, 2006. **40**(23): p. 2113-2130.
9. Owusu-Ansah, P., H. Yefa, and A. Misbawu. *Rotor Dynamic Modeling and Analysis of a Flywheel Rotor*. in *Proceedings of the 2015 International Conference on Electronic Science and Automation Control*. 2015. Atlantis Press.
10. Kale, V. and M. Secanell, *A comparative study between optimal metal and composite rotors for flywheel energy storage systems.* Energy Reports, 2018. **4**: p. 576-585.
11. Kress, G.R., *Shape optimization of a flywheel.* Structural and Multidisciplinary Optimization, 2000. **19**(1): p. 74-81.
12. Hou, Y., et al., *Size effect on mechanical properties and deformation behavior of pure copper wires considering free surface grains.* Materials, 2020. **13**(20): p. 4563.